Front. Chem. China 2011, 6(4): 358–366
DOI 10.1007/s11458-011-0255-4

RESEARCH ARTICLE

Molecular structure and vibrational spectra of phenobaraitone by density functional theory and ab initio hartree-Fock calculations

Ruizhou ZHANG (✉)[1], Xiaohong LI[1] and Xianzhou ZHANG[2]

Quantum chemistry calculations have been performed using Gaussian03 program to compute optimized geometry, harmonic vibrational frequency along with intensities in IR and Raman spectra at RHF/6-31++G and B3LYP/6-31++G** levels for phenobarbitone ($C_{12}H_{12}N_2O_3$) in the ground state. The scaled harmonic vibrational frequencies have been compared with experimental FT-IR and FT-Raman spectra. Theoretical vibrational spectra of the title compound were interpreted by means of potential energy distributions (PEDs) using MOLVIB program. A detailed interpretation of the infrared spectra of the title compound is reported. On the basis of the agreement between the calculated and observed results, the assignments of fundamental vibrational modes of phenobarbitone were examined and some assignments were proposed. The theoretical spectrograms for FT-IR and FT-Raman spectra of the title compound have been constructed.**

Keywords phenobarbitone, vibrational spectra, HF ab initio calculation, density functional theory (DFT)

1 Introduction

Phenobarbitone, a barbiturate, is used to control epilepsy and as a sedative to relieve anxiety. Phenobarbitone is 5-ethyl-5-phenylbarbituric acid and its molecular formula is $C_{12}H_{12}N_2O_3$. A general model compound with anticonvulsant activity proposed in Ref. [1] comprises two aromatic rings or their equivalents in a suitable orientation and a third, heterocyclic region, usually a cyclic imid. Williams [2] has reported the crystal structure of phenobarbitone. Recent spectroscopic studies of benzene and its derivatives have been motivated by their biologic and pharmaceutical importance [3,4]. The vibrational spectroscopic studies on benzene ring fused to five-membered received considerable attention recently [5–7]. The results obtained from these studies reveal that the change of simple constituents on a constant ring system produces only little changes in the spectrum. Gunasekaran et al. [8] recorded the infrared spectra of phenobarbitone in the region 4000–400 cm^{-1}, and Raman spectra in the region 3500–50 cm^{-1}. But so far no theoretical work is done on vibrational spectra of phenobarbitone because of the high complexity and low symmetry. Therefore, we made a deep investigation and studied the structure and vibrational frequencies of phenobarbitone.

Density functional theory (DFT) approaches, especially those using hybrid functional, have evolved to a powerful and very reliable tool, being routinely used for the determination of various molecular properties. B3LYP functional has been previously shown to provide an excellent compromise between accuracy and computational efficiency of vibrational spectra for large and medium size molecules [9–12]. It is well known that vibrational frequencies obtained by quantum chemical calculations are typically larger than their experimental counterparts, and thus, empirical scaling factors are usually used to match the experimental vibrational frequencies [13]. These scaling factors depend on both the method and basis sets used in calculations, and they are determined from the mean deviation between the calculated and experimental frequencies [14,15]. On the other hand, B exchange functionals have the advantage of standard frequency scaling factor which is very close to unity, so the B-based procedures can often be used without scaling [14,16–18]. For this reason, by using the DFT (B3LYP) method with B3LYP/6-31++G** basis set, we have calculated the geometric parameters and the vibrational spectrum of phenobarbitone in the ground state and compared with the experimental vibrational frequencies. The 6-31++G** basis set was also used for Hartree–Fock computations. These calculations are expected to provide new insight into the vibrational spectrum and molecular parameters.

The present study was undertaken with the following twofold objectives. One is to predict the IR and Raman spectra of the title compound. The other is to assign all predicted frequencies using normal mode analysis.

Received September 27, 2011; accepted October 12, 2011
1. College of Physics and Engineering, Henan University of Science and Technology, Luoyang 471003, China
2. College of Physics and Information Engineering, Henan Normal University, Xinxiang 453007, China
E-mail: lorna639@126.com

2 Computational details

Calculations of structural parameters, vibrational frequencies, IR and Raman intensities of the title compound (Fig. 1) were carried out using Gaussian03 program package [19] through RHF and DFT approaches.

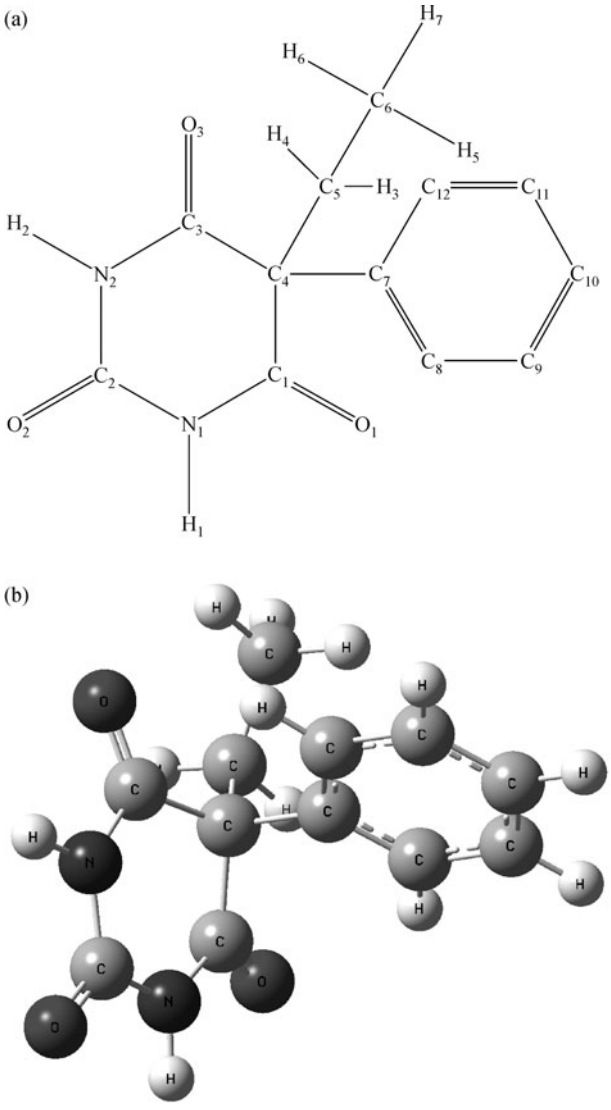

Figure 1 (a) The atom numbering scheme of phenobarbitone; (b) the optimized structure of phenobarbitone

Initially, the geometry optimization and calculation of other parameters were performed at restricted Hartree-Fock (RHF) level using 6-31++G** basis set. Electron correlations were included using Becke3-Lee-Yang-Parr (B3LYP) procedure [20–22]. This includes Becke's gradient exchange corrections, Lee, Yang and Parr correlation functional and/or Vosko, Wilk and Nusair correlation functional [23]. The optimized geometry at RHF/6-31++G** level was taken as the input structure for the density functional calculation at B3LYP/6-31++G** level. All the parameters were allowed to relax and all the calculations converged to an optimized geometry which corresponds to a true energy minimum revealed by the lack of imaginary frequencies. The vibrational frequencies for this molecule were calculated with the RHF and B3LYP methods with 6-31++G** basis set and then were scaled [24] by 0.8992 and 0.9614, respectively.

Furthermore, theoretical vibrational spectra of the title compound were interpreted by means of potential energy distribution (PED) with the version V7.0-G77 of the MOLVIB program written by Sundius [25,26].

The calculated Raman activity (S_i) have been converted to relative intensities (I_i) using the following relationship derived from the basis theory of Raman scattering [27,28]:

$$I_i = \frac{f(v_0 - v_i)^4 S_i}{v_i\left[1 - \exp\left(\frac{-hcv_i}{kT}\right)\right]} \quad (1)$$

where v_0 is the exciting frequency (in cm^{-1} units); v_i is the vibrational wavenumber of the ith normal mode; h, c and k are universal constants, and f is the suitably chosen common scaling factor for all the peak intensities.

3 Results and discussion

Williams [2] determined the crystal structure of the title compound. The title compound, $C_{12}H_{12}N_2O_3$, is monoclinic crystal system with the space group $P2_1/c$. The lattice parameters of the title compound are a = 9.534 Å, b = 11.855 Å, c = 10.794 Å, β = 111.56°, and Z = 4, D_c = 1.38.

3.1 Molecular geometry

The atom numbering scheme of the title compound is shown in Fig. 1 and the optimized geometrical parameters, namely, bond lengths and angles at RHF/6-31++G** and B3LYP/6-31++G** levels are given in Table 1. The experimental data obtained by Gunasekaran et al. [8] and Williams [2] are also included. It is noted from Table 1 that the bond lengths obtained by Gunasekaran et al. [8] and Williams [2] are not the same. The largest difference between them is 0.018 Å, while the bond angles obtained by them are nearly the same. Considering the different experimental methods, here, we adopted the experimental parameters obtained by Gunasekaran et al. [8].

The largest difference between experimental and calculated bond length by B3LYP method is about 0.031 Å. The RHF method leads to geometry parameters which are much closer to experimental data [2,8]. Optimized structure yields identical bond lengths for the N_1–C_2 and C_2–N_2, C_1–N_1 and C_3–N_2 bonds at the two levels of calculations RHF/6-31++

Table 1 Optimized geometrical parameters of phenobarbitone with 6–31++G** basis set

Bond length/Å	RHF	B3LYP	Exp.[a]	Exp[b]	Bond angle/°	RHF	B3LYP	Exp.[a]	Exp[b]
C_1–N_1	1.378	1.392	1.376	1.369	C_1–N_1–C_2	127.4	127.8	125.5	125.7
C_2–N_1	1.373	1.390	1.359	1.377	N_1–C_2–O_2	122.8	123.1	–	121.8
C_2–N_2	1.372	1.389	1.362	1.374	C_2–N_2–C_3	127.1	127.4	125.3	125.8
C_3–N_2	1.377	1.390	1.374	1.369	N_1–C_2–N_2	114.2	113.6	–	116.3
C_3–C_4	1.537	1.545	1.515	1.525	N_2–C_3–C_4	116.5	116.3	–	117.8
C_1–C_4	1.530	1.536	1.521	1.528	N_2–C_2–O_2	122.9	123.2	121.5	121.9
C_4–C_5	1.554	1.561	1.538	1.551	N_2–C_3–O_3	120.0	123.6	120.2	120.2
C_5–C_6	1.554	1.561	–	1.519	C_2–N_1–H_1	119.5	119.3	120.0	–
C_4–C_7	1.551	1.556	1.545	1.543	C_1–N_1–H_1	116.5	116.3	115.0	–
C_7–C_8	1.390	1.404	–	1.385	C_3–C_4–C_5	110.6	108.2	–	110.1
C_8–C_9	1.387	1.394	–	1.387	C_3–C_4–C_7	109.0	106.3	–	108.4
C_9–C_{10}	1.382	1.395	–	1.371	C_1–C_4–C_5	108.6	110.6	–	110.6
C_{10}–C_{11}	1.385	1.394	–	1.371	C_1–C_4–C_7	106.2	108.9	–	106.2
C_{11}–C_{12}	1.383	1.396	–	1.392	C_5–C_4–C_7	112.0	111.5	109.9	110.0
C_{12}–C_7	1.394	1.402	–	1.387	N_1–C_1–C_4	116.5	116.3	–	117.6
N_1–H_1	0.999	1.015	0.910	–	C_4–C_5–C_6	116.6	116.6	–	114.6
N_2–H_2	0.999	1.014	0.940	–	C_4–C_7–C_8	122.2	121.9	–	122.3
C_1–O_1	1.190	1.216	1.205	1.206	C_4–C_7–C_{12}	119.3	119.5	–	119.2
C_2–O_2	1.189	1.213	1.231	1.221	C_8–C_7–C_{12}	118.5	118.6	–	118.5
C_3–O_3	1.190	1.216	1.209	1.216	C_7–C_8–C_9	120.7	120.6	–	120.1
					C_8–C_9–C_{10}	120.4	120.4	–	121.3
					C_9–C_{10}–C_{11}	119.3	119.3	–	118.9
					C_{10}–C_{11}–C_{12}	120.4	120.4	–	120.7
					C_7–C_{12}–C_{11}	120.7	120.6	–	120.4
					C_1–C_4–C_3	110.3	111.2	110.7	111.4
					C_2–N_2–H_2	119.7	119.4	120.0	–
					C_3–N_2–H_2	116.6	116.4	115.0	–
					C_4–C_3–O_3	123.5	123.6	123.2	122.0
					C_4–C_1–O_1	123.8	124.0	123.4	122.2
					O_1–C_1–N_1	119.7	119.6	120.5	120.1

a) From Ref. [8]; b) From Ref. [2]

G** and B3LYP/6-31++G**, respectively. These bond lengths increase from RHF/6-31++G** to B3LYP/6-31++G** level and are found to be about 1.372 Å at RHF/6-31++G** level for phenobarbitone, which is between double bond length (C = N, 1.28 Å) and single (C–N, 1.47 Å) bond lengths.

Similarly, calculated C–O bond length increases from RHF to B3LYP level. The C–O bond lengths calculated by B3LYP level are closer to the experimental data [2,8]. The C_2–O_2 bond length is slightly shorter than the C_1–O_1 and C_3–O_3 bond lengths, which is probably due to the participation of O_1 and O_3 in intermolecular hydrogen bonds. The three C–O bond lengths are found to have a magnitude of about 1.213 Å between double (C = O, 1.20 Å) and single (C–O, 1.43 Å) bond length at B3LYP/6-31++G** level, which indicates its involvement in conjugation. The N–H bond lengths increase with the increase of the level of calculation refinements. The two N–H bond lengths are similar.

In bond angle calculation of phenobarbitone, the bond angles of C_1–N_1–C_2 and C_2–N_2–C_3 increase from RHF to DFT method and are 127.4° and 127.1° at RHF/6-31++G** level, respectively. Interestingly, bond angles of N_1–C_1–O_1 and C_4–C_1–O_1 are 119.7° and 123.8° at RHF/6-31++G** level, respectively, which indicates that the C_1= O_1 bond is not symmetrically disposed on C_1, rather, it is tilted toward the H_1 atom of the N_1–H_1 bond due to the propensity of O_1 atom to form H-bonding with the H_1 atom. Similarly, bond angles of N_2–C_3–O_3 and C_4–C_3–O_3 are 120.0° and 123.5° at RHF/6-31++G** level, respectively, which indicates that the C_3= O_3 bond is not symmetrically disposed on C_3, but tilted toward the H_2 atom of the N_2–H_2 bond due to the propensity of O_3 atom to form H-bonding with the H_2 atom.

Further, the bond angles of C_2–N_1–H_1 and C_1–N_1–H_1 are 119.5° and 116.5° at RHF/6-31++G** level, respectively. The magnitudes of these angles conform with the tilting of the N_1–H_1 bond toward oxygen atom of the C_1= O_1 bond to form

H-bonding. While the bond angles of C_2–N_2–H_2 and C_3–N_2–H_2 are 119.7° and 116.6° at RHF/6-31++G** level, respectively, which conforms with the tilting of the N_2–H_2 bond toward oxygen atom of the C_3=O_3 bond to form H-bonding. The hydrogen bond lengths and bond angles are listed in Table 2.

Table 2 The selected hydrogen bond lengths (Å) and bond angles (°) calculated by RHF/6-31 + + G** method

D-H..A	*d*(D-H)	*D*(H…A)	*D*(D…A)	∠DHA
N_1-H_1…O_1	0.999	2.45	2.258	65.368
N_2-H_2…O_3	0.999	2.49	2.256	64.370

All the dihedral angles on the benzene ring are either 0° or 180° with ± 1.0° at RHF/6-31++G** level, which indicates that the hydrogen atoms are in the plane of the benzene ring. The dihedral angles of C_8–C_7–C_4–C_1 and C_{12}–C_7–C_4–C_1 are 0° and 180°, respectively. The dihedral angles of C_8–C_7–C_4–C_3 and C_{12}–C_7–C_4–C_3 are −118.65° and 61.38°, respectively. The N_1, N_2, C_2, O_2 atoms are the planar part of the heterocyclic ring of the molecule. If the normal to the planar part of the heterocyclic ring is defined as the base vector of a spherical coordinate system, then the coordinate of the normal to the phenyl ring is $\varphi = 83.07°$, $\theta = 32.5°$.

In addition, the heterocyclic ring of the molecule is markedly non-planar. It is noted that the dihedral angles of O_2–C_2–N_1–C_1, C_2–N_1–C_1–O_1, O_2–C_2–N_2–C_3 and C_2–N_2–C_3–O_3 are 172.3°, −167.4°, −172.3° and 167.4°. The dihedral angles of C_2–N_2–C_3–C_4 and C_2–N_1–C_1–C_4 are 12.6° and −12.7°, respectively. The above analysis shows that the heterocyclic ring of the molecule assumes the characteristic "envelop" conformation.

3.2 Atomic charges

Mullican atomic charges at heterocyclic ring of phenobarbitone calculated at RHF/6-31++G** and B3LYP/6-31++G** levels are collected in Table 3. The magnitudes of charges calculated on N_1 and N_2 atoms increase from RHF to DFT level of calculation. Their values are found to be −0.66 and −0.67 at the B3LYP/6-31++G** level of calculation, respectively. The charges on H_1 and H_2 atoms exhibit positive charges and their magnitudes decrease from RHF to DFT method and are all 0.36 at DFT level of calculation.

The charge distribution listed in Table 3 shows that the double bond carbon atoms are negative except C_7 atom, whereas the remaining carbons are positively charged. The nitrogen atoms have more negative charges whereas all hydrogen atoms have positive charges. The result suggests that the atoms bonded nitrogen atoms are the electron acceptor, and also indicates that the charge transfers from H to N.

3.3 Vibrational analysis

The goal of the vibrational analysis is to find vibrational modes connected with specific molecular structures of calculated compound. To obtain the spectroscopic signature of phenobarbitone, vibrational frequencies were calculated by using RHF/6-31++G** and B3LYP/6-31++G** methods. The theoretically calculated DFT force fields were transformed to the latter set of vibrational coordinates and used in all subsequent calculations. Table 4 presents the calculated vibrational frequencies, IR intensities and Raman activity of phenobarbitone. The vibrational frequencies reported by S. Gunasekaran et al. [8] are listed in Table 4. The difference between experimental and calculated vibrational modes is observed. Any discrepancy noted between the observed and the calculated frequencies may be due to three facts: one is that hydrogen bond vibrations present in crystal lead to strong perturbation of the infrared frequencies (and intensities) of many other modes; one is that the experimental results belong to solid phase, and theoretical calculations belong to gaseous phase; the other is that the calculations have been actually done on a single molecule contrary to the experimental values recorded in the presence of intermolecular interactions.

Table 4 shows that the theoretical frequencies obtained with

Table 3 Atomic charges for optimized geometry of phenobarbitone

Atom no.	HF/6-31++G**	B3LYP/6-31++G**	Atom no.	HF/6-31++G**	B3LYP/6-31++G**
C_1	0.83	0.61	H_1	0.43	0.36
C_2	1.03	0.77	H_2	0.43	0.36
C_3	0.85	0.64	C_7	0.00	0.12
C_4	−0.30	−0.18	C_8	−0.21	−0.17
N_1	−0.90	−0.66	C_9	−0.20	−0.13
N_2	−0.91	−0.67	C_{10}	−0.20	−0.12
O_1	−0.56	−0.48	C_{11}	−0.20	−0.14
O_2	−0.58	−0.47	C_{12}	−0.22	−0.17
O_3	−0.57	−0.48			

Table 4 Calculated and experimental fundamental frequencies (cm^{-1}) for phenobarbitone

	Calculated frequencies		Experimental[a)] (IR)	Assignments[PED]
	HF/6-31++G**	B3LYP/6-31++G**		
1	405(0.09,0.22)	401(0.05,0.29)		Φ(ring)[95]
2	438(2.19,1.93)	432(2.80,2.86)		Φ(ring)[57]
3	485(7.07,1.72)	482(9.32,2.57)		δ(N–C = O)[45], Φ(ring) [34]
4	495(2.48,2.92)	491(1.45,2.68)		Φ(ring)[77]
5	540(50.51,1.90)	536(40.82,2.20)	560	δ(C–C–C) [38], Φ(ring)[54]
6	604(4.18,1.52)	609(2.47,2.64)		$\delta(N–H)_{oop}$ [39], α(ring)[51]
7	609(12.13,5.45)	613(3.70,11.58)	618	δ(C–C–C) [35], α(ring)[47]
8	617(3.01,9.58)	619(8.56,5.54)		$\delta(N–H)_{oop}$[75]
9	642(137.62,2.20)	655(59.41,2.42)		$\delta(N–H)_{oop}$[72]
10	668(2.47,1.04)	660(22.28,1.54)	672	δ(C–C = O)[52], $\delta(N–H)_{oop}$ [37]
11	694(0.74,1.00)	689(21.75,1.05)		$\delta(C–H)_{oop}$[90]
12	696(46.51,1.97)	693(17.07,1.55)		δ(N–C = O) [41],α(ring)[50]
13	713(34.67,2.10)	706(28.96,1.31)	693	δ(C–C = O)[65], $\delta(C–H)_{oop}$ [31]
14	739(2.18,0.48)	719(2.81,0.32)	716	δ(N–C = O)[88]
15	752(37.89,0.77)	722(100.55,0.29)	752	δ(N–C = O)[85]
16	761(127.23,0.57)	742(27.32,1.81)		$\delta(C–H)_{oop}$[76]
17	779(33.25,0.84)	769(16.74,1.28)		$\delta(C–H)_{oop}$[61],$\delta(C–H)_{ethyl}$ [29]
18	860(0.68,2.06)	834(0.58,4.08)		$\delta(C-H)_{oop}$[95]
19	914(8.64,9.06)	897(2.05,6.35)		$\delta(C-H)_{oop}$[62],$\delta(C-H)_{ethyl}$ [27]
20	937(7.28,2.69)	905(2.39,1.32)		$\delta(C–H)_{oop}$[85]
21	944(6.02,5.92)	940(10.18,4.97)		$\delta(C–H)_{methyl}$[71]
22	960(1.72,1.80)	945(0.66,0.47)		$\delta(C–H)_{oop}$[95]
23	974(2.10,23.35)	956(3.08,2.73)		$\delta(C–H)_{oop}$[57], ν(C–C) [38]
24	995(0.71,0.27)	969(0.28,0.29)		$\delta(C–H)_{oop}$[90]
25	1005(8.46,1.63)	980(3.20,22.83)		α(ring)[95]
26	1013(2.43,3.95)	994(6.32,1.26)		ν(C–N)[90]
27	1015(3.05,7.31)	1024(5.03,18.02)		ν(ring)[85]
28	1066(6.04,2.07)	1059(7.38,7.74)		ν(C–C)[69]
29	1074(13.83,7.13)	1080(8.21,1.97)		$\delta(C–H)_{ip}$[52],$\delta(C–H)_{methyl}$ [32]
30	1081(2.73,2.65)	1084(5.35,0.73)		$\delta(C–H)_{ip}$ [35],$\delta(C–H)_{methyl}$ [41]
31	1087(10.61,2.56)	1120(5.91,7.91)		$\delta(C–H)_{ip}$ [25],$\delta(C–H)_{methyl}$ [31],ν(C–C) [32]
32	1133(5.67,3.24)	1146(5.34,6.23)	1224	$\delta(C–H)_{ip}$ [28], $\delta(C–H)_{methyl}$ [34], ν(C–C) [30]
33	1167(4.47,2.89)	1154(0.53,4.64)		$\delta(C–H)_{ip}$[93]
34	1186(2.53,5.44)	1177(32.56,1.18)		ν(C–N)[50], $\delta(C–H)_{methyl}$ [37]
35	1189(9.02,2.63)	1188(4.17,7.16)		$\delta(C–H)_{ip}$[95]
36	1215(41.77,2.34)	1281(35.30,5.08)	1236	ν(C = C)[47], $\delta(C–H)_{ethyl}$[43]
37	1295(78.26,6.43)	1290(195.52,1.33)	1300	ν(C = C) [38], ν(C–N)[45]
38	1318(362.51,0.62)	1303(115.71,3.88)	1315	ν(C = C) [28], $\delta(C–H)_{ethyl}$ [30],ν(C–N) [34]
39	1338(29.74,0.58)	1331(12.35,0.46)		$\delta(C–H)_{ip}$[90]
40	1354(4.25,0.55)	1337(4.63,0.58)		$\delta(C–H)_{ethyl}$[84]
41	1380(58.99,0.19)	1350(12.89,0.48)	1350	$\delta(N–H)_{ip}$[45], ν(C–N) [32]
42	1402(10.67,1.88)	1377(217.27,3.48)	1368	ν(C-N)[72]
43	1414(227.44,3.02)	1387(20.54,1.95)		$\delta(C-H)_{methyl}$[77]
44	1430(104.11,4.60)	1396(84.07,3.57)		$\delta(N-H)_{ip}$[42], ν(C-N) [38]
45	1442(5.79,1.22)	1440(6.36,1.80)		$\delta(C–H)_{ip}$[80]
46	1464(3.38,16.36)	1462(4.08,13.71)		$\delta(C–H)_{methylene}$[87]
47	1468(6.17,16.81)	1471(5.28,19.58)		$\delta(C–H)_{methyl}$[75]
48	1482(2.94,5.68)	1488(11.25,2.17)		$\delta(C–H)_{methyl}$ [30], ν(C = C)[57]
49	1495(23.14,0.73)	1490(11.12,5.86)	1497	$\delta(C–H)_{ethyl}$[80]
50	1591(1.61,7.04)	1579(2.03,6.26)		ν(C = C)[87]

(*Continued*)

	Calculated frequencies		Experimental[a)] (IR)	Assignments[PED]
51	1614(4.35,24.79)	1598(4.90,29.99)		ν(C = C)[90]
52	1775(439.67,8.91)	1722(297.02,7.75)	1678	ν(C = O)[87]
53	1797(912.22,3.38)	1753(370.42,17.65)	1712	ν(C = O)[83]
54	1818(317.63,28.88)	1785(476.95,40.82)		ν(C = O)[85]
55	2874(37.47,70.92)	2944(23.55,101.56)		$\nu(C–H)_{methylene}$[90]
56	2880(29.89,177.32)	2951(28.20,143.46)		$\nu(C–H)_{methyl}$[95]
57	2927(48.73,61.09)	3006(3.82,50.10)		$\nu(C–H)_{ethyl}$[100]
58	2948(4.84,48.10)	3009(34.83,58.09)		$\nu(C–H)_{ethyl}$[100]
59	2978(15.18,16.37)	3051(9.59,18.01)		$\nu(C–H)_{ethyl}$[100]
60	3003(0.02,51.19)	3069(0.06,53.27)		$\nu(C–H)_{phenyl}$[100]
61	3013(16.48,100.82)	3079(14.53,110.57)		$\nu(C–H)_{phenyl}$[99]
62	3025(30.18,136.86)	3091(22.85,143.99)		$\nu(C–H)_{phenyl}$[100]
63	3040(7.67,51.65)	3103(6.01,7.48)		$\nu(C–H)_{phenyl}$[100]
64	3042(2.01,114.60)	3105(4.28,172.30)		$\nu(C–H)_{phenyl}$[100]
65	3432(136.48,46.85)	3460(81.24,76.38)	3207	ν_s(N–H) [100]
66	3435(88.39,95.18)	3463(60.45,129.62)	3308	ν_{as}(N–H) [100]

First numbers in the parentheses under the columns 2–3 correspond to the IR intensities and the second numbers to the Raman intensities. α: planar ring deformation; Φ: non-planar ring deformation; ν: stretching; δ: bending; ip: in-plane deformation; oop: out-of-plane deformation; ν_{ss}: symmetric stretching, ν_{ass}: asymmetric stretching.
a) Data from Ref. [8].

B3LYP method are in good agreement with their experimental data. While almost all the vibrations at RHF method deviate enormously even after scaling because of the single determinant wave function and the neglect of electron correlation. So discussions are being performed with the results at DFT level calculation with 6-31++G** basis set. Figs. 2 and 3 give the experimental and theoretical FT-IR and FT-Raman vibrational spectra of the title compound, respectively. Calculated Raman activities and IR intensities help us to distinguish and more precisely assign those fundamentals which are close in frequency.

3.3.1 C–H vibrations

The existence of one or more aromatic rings in a structure is normally readily determined from the C–H and C=C–C ring related vibrations. The C–H stretching occurs above 3000 cm^{-1} and is typically exhibited as a multiplicity of weak to moderate bands, compared with the aliphatic C–H stretch [29]. According to Roeges [30], the CH stretching vibrations of the phenyl ring are expected in the region of 3120–3000 cm^{-1}. The calculated values of these modes for phenobarbitone are 3069, 3079, 3091, 3103, 3105 cm^{-1} at B3LYP level. Experimentally, no bands are observed in the IR spectrum for phenobarbitone.

The C–H out of plane deformation is observed between 1000 and 700 cm^{-1} [30]. These δ(C–H) out of plane modes and δ(C–H) in-plane deformation vibration are not observed for phenobarbitone in the IR spectrum. The DFT

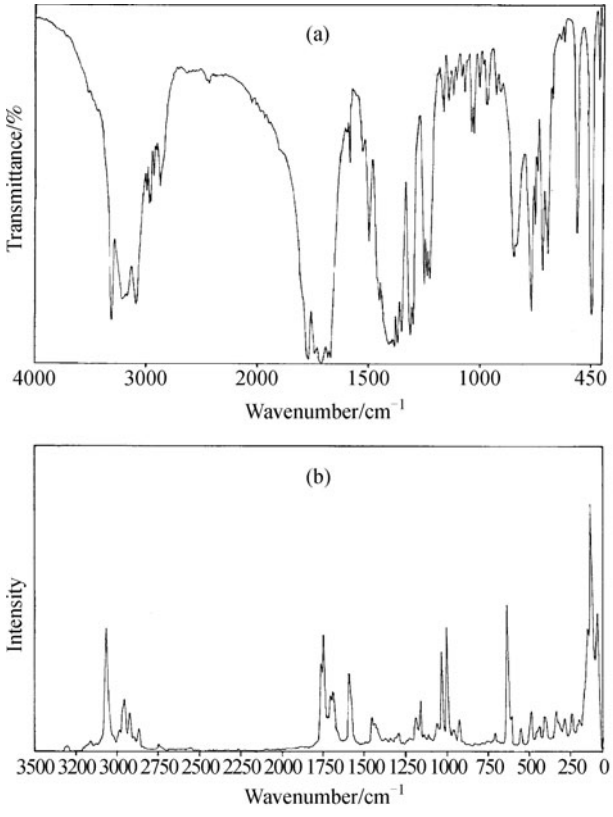

Figure 2 (a) The experimental FT-IR vibrational spectra of phenobarbitone; (b) the experimental FT-Raman vibrational spectra of phenobarbitone

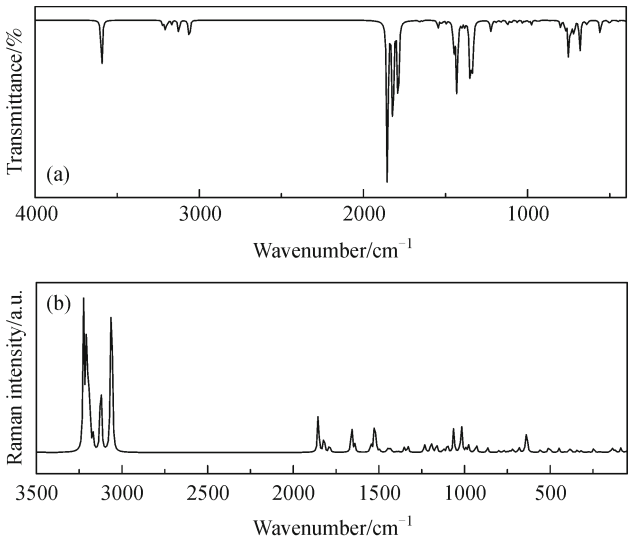

Figure 3 (a) The calculated FT-IR vibrational spectra of phenobarbitone by B3LYP method; (b) the calculated FT-Raman vibrational spectra of phenobarbitone by B3LYP method

calculations give $\delta(C–H)_{oop}$ at 689, 706, 742, 769, 834, 897, 905, 945, 956, 969 cm^{-1} and $\delta(C–H)_{ip}$ at 1080, 1084, 1120, 1146, 1154, 1188, 1331, 1440 cm^{-1} at B3LYP/6-31++G** method.

3.3.2 C–C stretching vibrations

The ring carbon-carbon stretching vibrations occur in the region 1625–1430 cm^{-1}. For aromatic six-membered rings, e.g., benzenes and pyridines, there are two or three bands in this region due to skeletal vibrations, the strongest usually being at about 1500 cm^{-1}. For substituted benzenes with identical atoms or groups on all para-pairs of ring carbon atoms, the vibrations causing the band at 1625–1590 cm^{-1} are infrared-inactive due to symmetry consideration; the compound has a center of symmetry at the ring center. If there is no center of symmetry, the vibrations are infrared-active [31]. Chithambarathau et al. [32] have observed the FT-IR bands at 1574, 1498 and 1468 cm^{-1} in 1,3,5-triphenyl-4,5-dihydro pyrazole. In the present work, the CC stretching is observed at 1236 cm^{-1} for phenobarbitone in the IR spectrum [8]. The DFT calculations give the aromatic CC stretching modes at 1281, 1290, 1303, 1488, 1579, 1598 cm^{-1}.

3.3.3 C–N vibrations

The weak absorption bands for the C–N linkages in amines appear in the region 1200–1020 cm^{-1}. It is a difficult task to identify the C–N stretching in the side chain from other vibrations [33]. The ring C = C and C = N stretching vibrations occur in the region 1615–1575 cm^{-1} and 1520–1465 cm^{-1} [34]. Krishnakumar and Xavier [35] have observed the C–N stretching vibration at 1375 cm^{-1} in pyrimidines. Mohan et al. [36] have identified the stretching frequency of C = N bond in benzimidazole at 1617 cm^{-1}. For phenobarbitone, C–N stretching vibrations are observed at 1315, 1350, 1368 cm^{-1} [8]. DFT calculations give the C–N stretching vibrations at 994, 1290, 1303, 1350, 1377, 1396 cm^{-1}.

3.3.4 C = O vibration

The carbonyl group is important and its characteristic frequency has been extensively used to study a wide range of compounds. The carbonyl group vibrations give rise to characteristic bands in vibrational spectra. The intensity of these bands can increase owing to conjugation or formation of hydrogen bonds. The increase in conjugation, therefore, leads to intensification of IR bands. If a compound contains a carbonyl group, the absorption caused by C = O stretching is generally the strongest peak [33]. The C = O stretching frequency appears strongly in the infrared spectrum in the range 1600–1850 cm^{-1}. The C = O stretching modes reported by S.Gunasekaran et al. [8] are 1678 and 1712 cm^{-1}. DFT calculation gives C = O stretching modes at 1722, 1753, 1785 cm^{-1}. The deviation of the calculated wavenumber for this mode can be attributed to the underestimation of the large degree of π-electron delocalization due to the conjugation in the molecule [37].

3.3.5 N–H vibration

The NH stretching vibration [30] appears strongly and broadly in the region of (3390±60) cm^{-1}. For the title compound, the N–H symmetric stretching reported by Gunasekaran et al. [8] is at 3207 cm^{-1}, and the N–H asymmetric stretching reported is at 3308 cm^{-1} in the IR spectrum. The calculated value for N–H symmetric stretching is 3460 cm^{-1}, and the N-H asymmetric stretching obtained is at 3463 cm^{-1}. The NH stretching wavenumber is red shifted by 155–253 cm^{-1} in the IR with a strong intensity from the computed wavenumber, which indicates that the weakening of the N_2–H_2 bond results in proton transfer to the neighboring oxygen [38].

3.3.6 Deformation vibrations

In benzene, six ring deformation frequencies are observed. Of these, three arise from in-plane bending vibrations corresponding to 606 and 1010 cm^{-1} mode, and the remaining three

are derived from out-of-plane bending vibrations corresponding to 404 and 711 cm^{-1} mode of vibrations. The in-plane bending mode of benzene splits into two components in substituted benzenes while both of these components are reducing heavily in metal isomers of di-substituted benzenes [39,40]. The aromatic ring vibration is not reported by S. Gunasekaran et al. [8]; the *v*(ring) mode is calculated at 1024 cm^{-1} for phenobarbitone. DFT calculations give the α (ring) vibrational modes at 609, 613, 693, 980 cm^{-1} and Φ(ring) vibrational modes at 401, 432, 482, 491, 536 cm^{-1}.

3.3.7 Hydrogen bonding

Generally, a hydrogen bond is formed when the hydrogen atom of a covalent A-H bond of a proton donor molecule interacts with a lone electron pair of an atom of X of a proton acceptor. In the title compound, there exist some hydrogen bonds. Among these, there is one hydrogen bond of the N–H…O type. The intramolecular H…O distances of H_1–O_1 is found to be 2.45 Å. These distances are much shorter than that of the van der Waals separation between the O atom and H atom (2.72 Å) [41] indicating the existence of the N–H…O interaction in the title compound. The DFT calculation predicts the shortening of N_1–H_1 bond, and the bond length is 0.999 Å, which leads to red shift in their observed band in IR spectra.

3.4 Other molecular properties

Several calculated thermodynamic parameters are presented in Table 5. Scale factors have been recommended for an accurate prediction in determining the zero-point vibration energies (ZPVE), and the entropy, $S_{vib}(T)$. The variations in the ZPVEs seem to be insignificant. The total energies and the change in the total entropy of the title compound at room temperature at different methods are also presented.

Table 5 Theoretically computed energies (a.u.), zero-point vibrational energies (kcal·mol^{-1}), rotational constants (GHz), entropies (cal·mol^{-1}·K^{-1}) and dipole moment (*D*) for the title compound with 6-31++G** basis set

Parameters	RHF	B3LYP
Total energy	−794.717556	−799.501595
Zero-point energy	155.08101	144.14073
Rotational constants	0.64987, 0.41626, 0.38648	0.64444, 0.40548, 0.38035
$Entropy_{total}$	117.829	122.074
$Entropy_{translational}$	42.228	42.228
$Entropy_{rotational}$	32.397	32.447
$Entropy_{vibrational}$	43.204	47.399
Dipole moment	2.0577	1.5417

4 Conclusions

The optimized molecular structures, vibrational frequencies and corresponding vibrational assignments of phenobarbitone have been calculated using RHF/6-31++G** and B3LYP/6-31++G**. The analysis of the bond distance for the title compound shows that there exists the strong H-bonding between H_1 and O_1 atoms, and H_2 and O_3 atoms. A same conclusion is obtained from the analysis of the bond angle. The comparison of the experimental and calculated spectra of the molecules showed that DFT B3LYP method is in good agreement with experimental ones. Following the agreement between the calculated and experimental results, all the fundamental vibrational modes of the title compound were assigned based on the results of the PED output obtained from normal coordinate analysis.

Acknowledgements We would like to thank the National Natural Science Foundation of China (Grant No. 10774039), the Development Program in Science and Technology of Henan Province (No. 102300410114), and Henan University of Science and Technology for Young Scholars (No. 2009QN0032) for their support of this work.

References

1. Brown, M. L.; Brown, G. B.; Brouillette, W. J., *J. Med. Chem*. **1997**, *40*, 602–607
2. Williams, P. P., *Acta Crystallogr. B* **1974**, *30*, 12
3. Gunasekaran, S.; Thilak Kumar, R.; Periyanayagasamy, V.; Raihana, M. P.; *Asian J. Chem*. **2005**, *17*, 1211
4. Gunasekaran, S.; Ponnambalam, U.; Muthu, S.; Ponnusamy, S.; Asian, J., *Chem*. **2004**, *16*, 1513
5. Gunasekaran, S.; Ponnambalam, U.; Muthu, S., *Acta Ciencia Indica XXX*. **2004**, *1*, 15
6. Gunasekaran, S.; Ponnambalam, U.; Muthu, S.; Mariappan, L. *Asian. J. Phys*. **2003**, *16*, 51
7. Gunasekaran, S.; Shankari, G.; Ponnusamy, S., *Spectrochimica Acta Part A*. **2005**, *61*, 117–127
8. Gunasekaran, S.; Thilak Kumar, R.; Ponnusamy, S., *Spectrochimica Acta Part A*. **2006**, *65*, 1041–1052
9. Korth, H. G.; de Heer, M. I.; Mulder, P., *J. Phys. Chem*. **2002**, *106*, 8779
10. Chowdhury, P. K., *J. Phys. Chem. A* **2003**, *107*, 5692–5696
11. Chis, V., *Chem. Phys*. **2004**, *300*, 1–11
12. Asensio, A.; Kobko, N.; Dannenberg, J. J., *J. Phys. Chem. A* **2003**, *107*, 6441–6443
13. Jensen, F., *Introduction to Computational Chemistry*, Wiley, New York, 1999.
14. Rauhut, G.; Pulay, P., *J. Phys. Chem*. **1995**, *99*, 3093–3100
15. Sinha, P.; Boesch, S. E.; Gu, C.; Wheeler, R. A.; Wilson, A. K., *J. Phys. Chem A*. **2004**, *108*, 9213–9217

16. Scott, A. P.; Radom, L., *J. Phys. Chem*. **1996**, *100*, 16502–16513
17. Kolev, T. M.; Stamboliyskaya, B. A., *Spectrochimica acta Part A*. 2002, 58, 3127
18. Pfeiffer, M.; Baier, F.; Stey, T.; Leusser, D.; Stalke, D.; Engels, B.; Moigno, D.; Kiefer, W., *J. Mol. Model*. **2000**, *6*, 299–311
19. Frisch, M. J.; Trucks, G. W.; Schlegel, H. B.; Scuseria, G. E.; Robb, M. A.; Cheeseman, J. R.; Montgomery, J. A. Jr; Vreven, T.; Kudin, K. N.; Burant, J. C.; Millam, J. M.; Iyengar, S. S.; Tomasi, J.; Barone, V.; Mennucci, B.; Cossi, M.; Scalmani, G.; Rega, N.; Petersson, G. A.; Nakatsuji, H.; Hada, M.; Ehara, M.; Toyota, K.; Fukuda, R.; Hasegawa, J.; Ishida, M.; Nakajima, T.; Honda, Y.; Kitao, O.; Nakai, H.; Klene, M.; Li, X.; Knox, J. E.; Hratchian, H. P.; Cross, J. B.; Adamo, C.; Jaramillo, J.; Gomperts, R.; Stratmann, R. E.; Yazyev, O.; Austin, A. J.; Cammi, R.; Pomelli, C.; Ochterski, J. W.; Ayala, P. Y.; Morokuma, K.; Voth, G. A.; Salvador, P.; Dannenberg, J. J.; Zakrzewski, V. G.; Dapprich, S.; Daniels, A. D.; Strain, M. C.; Farkas, O.; Malick, D. K.; Rabuck, A. D.; Raghavachari, K.; Foresman, J. B.; Ortiz, J. V.; Cui, Q.; Baboul, A. G.; Clifford, S.; Cioslowski, J.; Stefanov, B. B.; Liu, G.; Liashenko, A.; Piskorz, P.; Komaromi, I.; Martin, R. L.; Fox, D. J.; Keith, T.; Al-Laham, M. A.; Peng, C. Y.; Nanayakkara, A.; Challacombe, M.; Gill, P. M. W.; Johnson, B.; Chen, W.; Wong, M. W.; Gonzalez, C.; Pople, J. A., Gaussian '03, Revision C. 01, Gaussian, Inc., Wallingford, CT, 2004
20. Becke, A. D., *J. Chem. Phys*. **1993**, *98*, 5648
21. Lee, C.; Yang, W.; Parr, R. G., *Phys. Rev. B* **1988**, *37*, 785–789
22. Becke, B. D., *Phys. Rev. B* **1988**, *38*, 3098
23. Vosko, S. H.; Wilk, L.; Nusair, M., *Can. J. Phys*. **1980**, *58*, 1200–1211
24. Fast, P. L.; Corchado, J.; Sanchez, M. L.; Truhlar, D. G., *J. Phys. Chem. A* **1999**, *103*, 3139–3143
25. T. Sundius, MOLVIB: A program for harmonic force field calculations, QCPE program No. 807, 2002
26. Sundius, T., *Vib. Spectrosc*. **2002**, *29*, 89–95
27. Keresztury, G.; Holly, S.; Varga, J.; Besenyei, G.; Wang, A. Y.; Durig, J. R., *Spectrochimica Acta Part A*. **1993**, *49*, 2007–2026
28. Keresztury, G.; Chalmers, J. M.; Griffith, P. R., *RamanSpectroscopy: Theory in Handbook of Vibrational Spectroscopy*, vol. 1, John Wiley & Sons Ltd., 2002, p127
29. Coates, J., in: R.A. Meyers (Ed.), *Interpretation of Infrared Spectra, A Practical Approach*, John Wiley and Sons Ltd., Chichester, 2000, p235
30. Roeges, N. P. G., *A Guide to Complete Interpretation of Infrared Spectra of Organic Structures*, Wiley, New York, 1994, p74
31. Socrates, G., *Infrared Characteristic Group Frequencies*, John Wiley, New York, 2000, p158
32. Chithambarathanu, T.; Umayourbaghan, V.; Krishnakumar, V., *Indian J. Pure Appl. Phys*. **2003**, *41*, 844
33. Nakkeeran, C., Thesis Ph.D, Bharathidasan University, Tiruchirappalli, Tamil Nadu, India, 1997.
34. Parasuraman, M., Thesis Ph.D, University of Madras, Chennai, India, 2001.
35. Krishnakumar, V.; John Xavier, R., *Indian J.Pure Appl. Phys.* **2003**, *41*, 597
36. Mohan, S.; Sundaraganesan, N.; Mink, J., *Spectrochimica Acta Part A.* **1991**, *47*, 1111–1115
37. Panicker, C. Y.; Varghese, H. T.; Philip, D. P.; Nogueira, H. I. S.; Kastkova, K., *Spectrochimica Acta Part A.* **2007**, *67*, 1313–1320
38. Barthes, M.; De Nunzio, G.; Riber, G., *Synth. Met*. **1996**, *76*, 337–340
39. Xavier Jesu Raja, S.; William, A.; Gunasekaran, S., *Orient J. Chem*. **1994**, *10*, 3
40. Marshell, J.; Gunasekaran, S., *Indian J. Phys. B* **1996**, *70*, 505
41. Sato, H.; Dybal, J.; Murakami, R.; Noda, I.; Ozaki, Y., *J. Mol. Struct*. **2005**, *35*, 744